



## OPEN The small molecule LOXL2 inhibitor SNT-5382 reduces cardiac fibrosis and achieves strong clinical target engagement

Lara Perryman<sup>1</sup>, Alison Findlay<sup>1</sup>, Jana Baskar<sup>1</sup>, Brett Charlton<sup>1</sup>, Jonathan Foot<sup>1</sup>, Ross Hamilton<sup>1</sup>, Dieter Hamprecht<sup>1</sup>, Amar Joshi<sup>1</sup>, Jessica Stolp<sup>1</sup>, Craig Turner<sup>1</sup>, Amna Zahoor<sup>1</sup>, Wenbin Zhou<sup>1</sup>, Begoña López<sup>2,3</sup>, Susana Ravassa<sup>2,3</sup>, Arantxa González<sup>2,3,4</sup> & Wolfgang Jarolimek<sup>1</sup>✉

Cardiac remodeling involves myocardial hypertrophy and fibrosis which impairs cardiac function and, ultimately, contributes to heart failure (HF) and mortality. Fibrosis largely develops due to excessive matrix deposition and lysyl oxidase(s)-dependent collagen cross-linking. In particular, lysyl oxidase-like 2 (LOXL2) has a critical role in disease progression, representing a promising therapeutic target and rationale for the development of novel, efficacious LOXL2 inhibitor(s). Herein, we describe the pre-clinical validation of a potent small molecule LOXL2 inhibitor as an anti-fibrotic agent, along with its clinical suitability, as high levels of target engagement were sustained in Phase 1 clinical trials while also being well tolerated. We show that LOXL2 concentration is increased in the plasma of patients with HF due to existing hypertension or aortic stenosis. Plasma LOXL2 concentration were correlated with the left ventricular mass index. A novel LOXL2 inhibitor, SNT-5382, was characterised, including *in vitro* and *in vivo* assessment of potency and mode of action, which showed beneficial drug-like properties. Preclinically, SNT-5382 reduced fibrosis and improved cardiac function in a myocardial infarction (MI) mouse model. Phase 1 clinical studies demonstrated a good safety and a PK profile capable of eliciting high and prolonged LOXL2 inhibition following repeated once daily oral dosing. Our findings underscore the pivotal role of LOXL2 in the development of HF. SNT-5382 exhibited potent anti-fibrotic efficacy in a MI model and sustained clinical target engagement.

**Trial registration:** Australian New Zealand Clinical Trials Registry identifier: ACTRN12617001564347. Registered 21 November 2017 - registered, <https://www.anzctr.org.au/Trial/Registration/TrialReview.aspx?ACTRN=12617001564347>

**Keywords** Heart failure, Lysyl oxidases, LOXL2 small molecule inhibitor, Anti-fibrotic therapy, Fibrosis

### Abbreviations

AS	Aortic stenosis
CVDs	Cardiovascular diseases
ECHO	Echocardiography
EDD	End-diastolic diameter
ESD	End-systolic diameter
EF	Ejection fraction
FS	Fractional shortening
HF	Heart failure
HT	Hypertension
IVSd	Interventricular septal thickness at end diastole
LVMI	Left ventricular mass index

<sup>1</sup>Syntara, Frenchs Forest, NSW, Australia. <sup>2</sup>Program of Cardiovascular Diseases, CIMA Universidad de Navarra and IdiSNA, Pamplona, Spain. <sup>3</sup>CIBERCV, Carlos III Institute of Health, Madrid, Spain. <sup>4</sup>Department of Cardiology and Cardiac Surgery, Clínica Universidad de Navarra, Pamplona, Spain. ✉email: Wolfgang.Jarolimek@Syntaratx.com.au

LVPWd	Left ventricular posterior wall thickness at end diastole
LVEDD	Left ventricle end diastolic diameter
LVESD	Left ventricle end systolic diameter
LTQ	Lysine tyrosylquinone
LOXs	Lysyl oxidases
LOXL2	Lysyl oxidase-like 2
MI	Myocardial infarction
NT-proBNP	Amino-terminal pro-brain natriuretic peptide
PD	Pharmacodynamic
PK	Pharmacokinetic
SAD	Single ascending dose
MAD	Multiple ascending dose

Cardiovascular diseases (CVDs) are a major risk factor for heart failure (HF) and remain the leading cause of mortality worldwide<sup>1</sup>. Aortic stenosis (AS) and hypertension (HT) are characterised by chronic pressure overload that leads to left ventricular remodeling<sup>2,3</sup>. Initially, the cardiac remodeling and hypertrophy serve as compensatory mechanisms to maintain cardiac function. However, as they progress over time, they contribute to the development of cardiac dysfunction and HF, unless therapeutic interventions occur.

Cardiac fibrosis is a major hallmark of cardiac remodeling and is a prognostic factor in HF. It can be an initial adaptive stress response to acute (myocardial infarction) or chronic conditions like cardiac pressure (hypertension) or volume overload. It contributes to a stiffening of cardiac chambers and the development of cardiac dysfunction<sup>4</sup>. The predominant extracellular matrix component in fibrosis is fibrillar collagen, with increasing levels of deposition, and cross-linking worsening the stiffness of cardiac tissue<sup>5</sup>. Highly cross-linked collagen is more resistant to degrading enzymes<sup>6</sup>. In HF patients, the degree of collagen cross-linking is increased<sup>7</sup> and is correlated with worsened diastolic dysfunction, higher left ventricular filling pressure and increased stiffness<sup>8–11</sup>, as well as a higher risk of rehospitalization for HF<sup>12</sup>. Furthermore, HT patients with increased left ventricular mass index (LVMI; a measure of left ventricular hypertrophy that is concomitant with the development of fibrosis<sup>13</sup>) have a high risk of HF and all-cause mortality<sup>14</sup>. While standard of care medications have proven invaluable for the treatment of HF, there remains a clear unmet clinical need for therapeutic interventions that specifically target the progression of fibrosis.

Lysyl oxidases (LOXs) are a family of enzymes that catalyse the formation of collagen cross-links, thereby playing a pivotal role in the progression of fibrosis<sup>15</sup>. Previous studies in experimental models of both chronic and acute cardiac fibrosis have highlighted the role of one particular family member, lysyl oxidase-like 2 (LOXL2), in left ventricular dysfunction<sup>16–18</sup>. Increased expression of LOXL2 has been found in patients with ischaemic or non-ischaemic dilated cardiomyopathy and in patients with HF with preserved ejection fraction<sup>16</sup>. Furthermore, HT patients at high risk of HF have elevated serum LOXL2 levels which were positively correlated with established CVD biomarkers [such as amino-terminal pro-brain natriuretic peptide (NT-proBNP), Troponin I] and cardiac dysfunction<sup>16</sup>.

The rationale for LOXL2 inhibition as an anti-fibrotic therapy has been established in both preclinical and clinical settings. In CVD animal models, decreases in LOXL2 activity achieved either by genetic deletion or by pharmacological intervention, caused a reduction in fibrosis, attenuation of the associated impairment in cardiac function<sup>16,17,19,20</sup> and improvements in survival<sup>21</sup>. Initial clinical proof-of-concept of the anti-fibrotic efficacy of LOXL2 inhibition has been achieved by the small molecule, GB2064, that reduced bone marrow collagen fibrosis grade in 60% of myelofibrosis patients treated for 9 months<sup>22</sup>. This success followed several high-profile clinical trial failures involving simtuzumab, an allosteric LOXL2 selective antibody. Initially, the disappointing results of simtuzumab in the clinics were attributed to the target being unsuitable, however it is now evident that the antibody did not inhibit the enzymatic activity of LOXL2<sup>23,24</sup>, reinstating LOXL2 as a highly relevant anti-fibrotic target.

Herein, we present further evidence in support of LOXL2 as an important therapeutic target in patients with HF. We also describe the development of a clinical candidate, SNT-5382, that capitalised on a sound understanding of the structure–activity relationships governing potency and selectivity. Moreover, we demonstrate good safety, pharmacokinetic properties and a high long-lasting target engagement following repeated once daily oral dosing in the clinic.

## Results

### LOXL2 is upregulated in chronic heart failure

In many fibrotic diseases, plasma LOXL2 concentration has been proposed as a diagnostic biomarker<sup>16,17,25–27</sup>. A digital ELISA analysis was utilized to measure LOXL2 plasma concentrations<sup>24</sup>. LOXL2 levels increased in AS patients with HF compared to control subjects ( $p < 0.05$ , Fig. 1A). This difference remained statistically significant after controlling for age, sex, body mass index and estimated glomerular filtration rate (ANCOVA,  $p < 0.05$ ) (Supplementary Fig. 1A).

To further substantiate the positive association of LOXL2 and HF, LOXL2 plasma levels were analyzed in hypertensive (HT) patients with or without HF. Again, patients with HF had higher plasma LOXL2 concentrations than those without ( $p < 0.001$ , Fig. 1B). This difference remained statistically significant after controlling for age and sex (ANCOVA,  $p < 0.001$ ) (Supplementary Fig. 11B). The elevated levels were similar in HF patients with either preserved ( $n = 11$ ) or reduced ejection fraction ( $n = 12$ ) ( $173 \pm 77$  vs.  $163 \pm 94$  pg/mL, respectively) and there was no sex difference (men:  $163 \pm 48$ . women:  $171 \pm 106$  pg/mL) (Supplementary Table 1: Patient demographics).

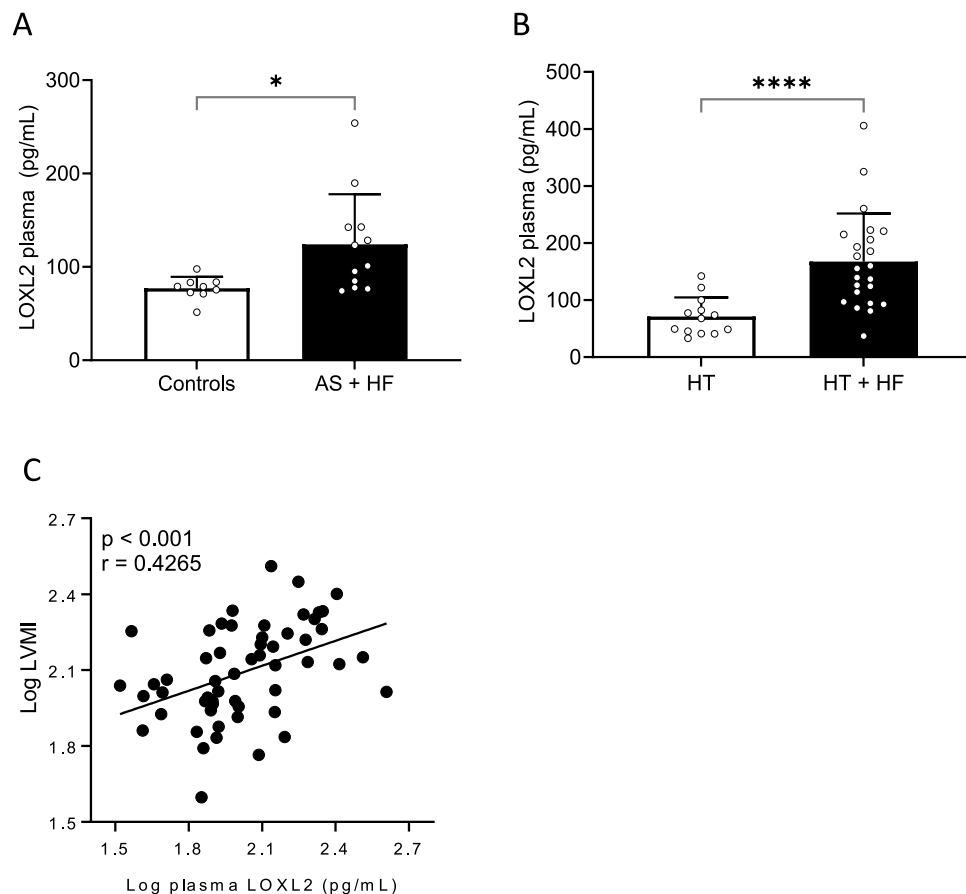


**Fig. 1.** LOXL2 concentrations in plasma from patients with heart failure. **(A)** LOXL2 plasma concentration in patients with aortic stenosis and heart failure (AS + HF,  $n = 12$ ) compared to control subjects ( $n = 9$ ). **(B)** The LOXL2 plasma concentration of hypertensive (HT) patients with ( $n = 23$ ) and without ( $n = 13$ ) HF. The data for A and B are expressed as the mean  $\pm$  standard deviation (SD) and analysed using a F-test, to test for equal variance, hence an unpaired two-tailed Student's t-test with a Welch correction was used. \* Indicates a significant difference  $*p < 0.05$ ,  $***p < 0.001$ . **(C)** Correlation of LOXL2 plasma concentration with the left ventricular mass index (LVMI) in patients with aortic stenosis, hypertensive patients with heart failure, hypertensive patients without heart failure and control subjects. Pearson correlation coefficient was used to determine the  $r$  and  $p$  value ( $n = 56$ ). LOXL2 and LVMI values were normalized by logarithmic transformation.

A positive correlation was found between plasma LOXL2 levels and LVMI, a parameter assessing left ventricular hypertrophy ( $r = 0.426$ ;  $p < 0.01$ , Fig. 1C) which was maintained after adjusting for age and sex ( $r = 0.325$ ;  $p < 0.01$ ).

### Development of a potent LOXL2 inhibitor, SNT-5382

Building upon previously published indole<sup>28</sup> and aza-indole-based<sup>29</sup> inhibitors, we developed SNT-5382 (Fig. 2A), a potent, selective LOXL2 inhibitor ( $IC_{50}$  10 nM) with favourable developability properties. SNT-5382 exhibits rapid, time-dependent LOXL2 inhibition (Fig. 2B) and competitively binds to the active site of the target enzyme (Supplementary Fig. 2).

Similar to other haloalkylamine-containing amine oxidase inhibitors<sup>30</sup>, the presence of the fluoro moiety is crucial in achieving irreversible inhibition, with the corresponding des-fluoro analogue readily displaced by the substrate in a jump dilution experiment (Fig. 2C) performed using human recombinant (hr) LOXL2. Based on these findings the postulated mechanism of LOXL2 inhibition by SNT-5382 is shown in Fig. 2E. SNT-5382 initially binds to the lysine tyrosylquinone (LTQ) cofactor within the enzymatic pocket, resulting in Schiff base formation and subsequent oxidation. Nucleophilic attack by an amino acid within the active site then leads to a covalently bound enzyme-inhibitor complex. While classical covalent inhibitors have reactive functional groups that can form adducts with off-target proteins (potentially leading to unwanted side effects) SNT-5382 is activated only upon binding to the LTQ co-factor within the active site of LOXL2.

To assess the selectivity of SNT-5382, we tested it against other lysyl oxidases, amine oxidases and macromolecules. At therapeutically relevant concentrations, SNT-5382 also inhibits LOXL3 ( $IC_{50}$  20 nM) and, to a lesser extent, LOXL4 ( $IC_{50}$  118 nM) (Fig. 2D). Both family members are increasingly recognised as important drivers in a host of fibrotic conditions<sup>31</sup>. In contrast, SNT-5382 exhibits good selectivity ( $> 80$ -fold) over the so-called housekeeping family members LOX ( $IC_{50}$  833 nM) and LOXL1 ( $IC_{50}$  1710 nM) (Fig. 2D). Moreover, the

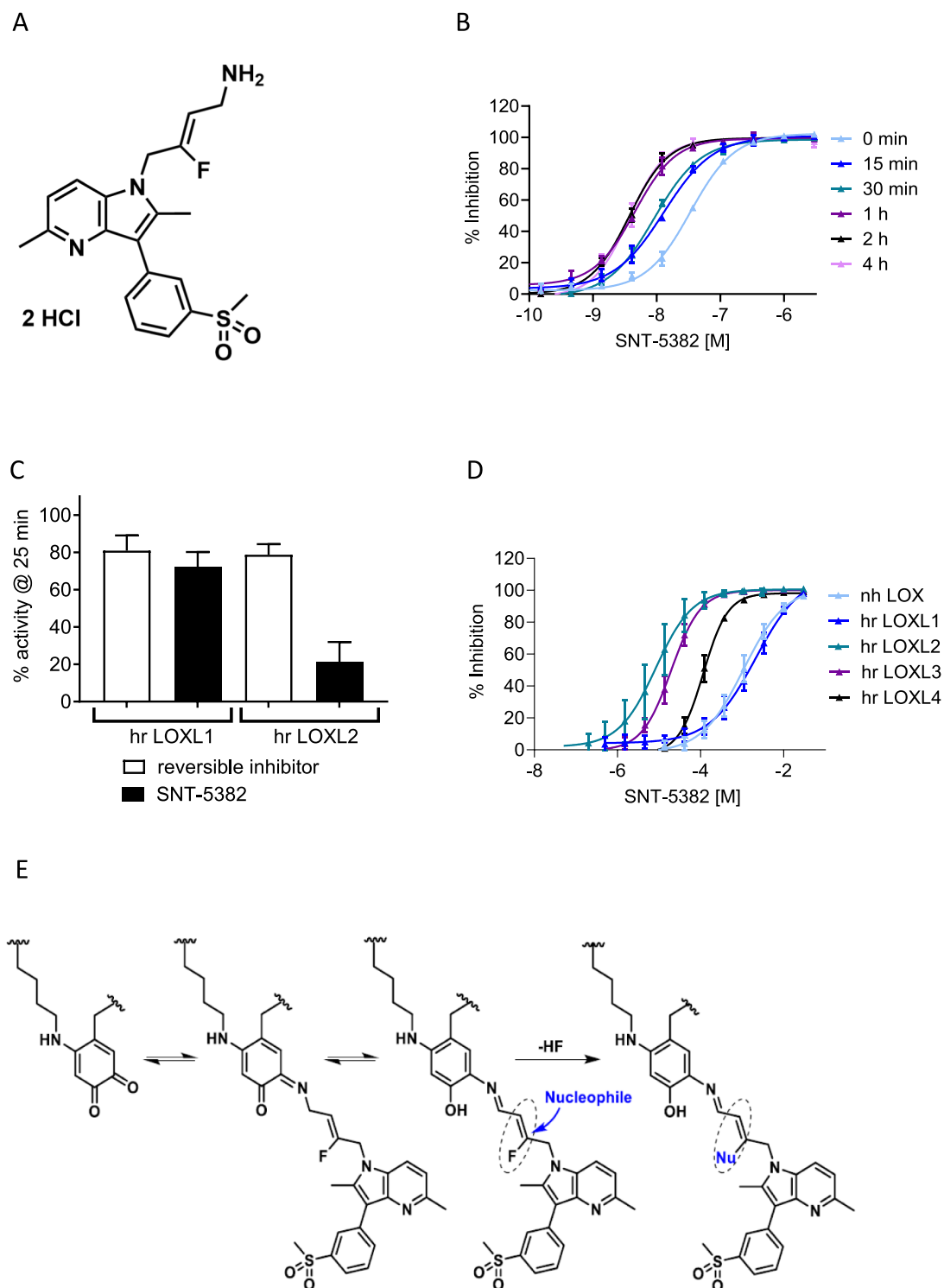


**Fig. 2.** SNT-5382 is an irreversible, mechanism-based inhibitor of LOXL2. **(A)** Chemical structure of SNT-5382. **(B)** The potency of human recombinant LOXL2 activity by SNT-5382 increases with pre-incubation. ( $n = 3$ ). **(C)** The irreversible binding of SNT-5382 measured in a jump dilution assay for both human recombinant (hr) LOXL2 and LOXL1. The reversible inhibitor is the des-fluoro analogue of SNT-5382. ( $n = 3$ ). **(D)** Concentration response curves of the inhibition of lysyl oxidase family enzymatic activity had a 30 min pre-incubation and measured using an Amplex Red oxidation assay, as described previously<sup>29</sup>; hn: human native; hr: human recombinant. ( $n = 3$ ). **(E)** Postulated mechanism of inhibition of SNT-5382. Data are presented as mean  $\pm$  SD.

margin of selectivity is increased by the reversible nature of SNT-5382 binding to hr LOXL1, as evidenced by results from the jump dilution assay (Fig. 2C). SNT-5382 has excellent selectivity over other amine oxidases and macromolecular targets (Supplementary Tables 2 and 3).

The *in vitro* and *in vivo* ADME characteristics of SNT-5382 were profiled in a series of standard assays. Plasma protein binding in humans, dogs and rats was low (Fig. 3A). SNT-5382 exhibits high plasma and metabolic (microsome and hepatocyte) stability across species. The compound does not show a significant propensity for drug-drug interactions. At therapeutically relevant concentrations, SNT-5382 does not block transporters or demonstrate significant irreversible inhibition of cytochrome P450 (CYP) enzymes, although moderate inhibition of CYP2C9 and 2C19 was observed (Supplementary table 4).

In rats, SNT-5382 is well absorbed after oral dosing as an aqueous solution (10 mg/kg) and reaches peak plasma concentrations approximately 3 h (h) later (Fig. 3B). Tissue concentrations of SNT-5382 increased from 1 to 4 h after oral administration and SNT-5382 was well distributed across all organs (Fig. 3C).

SNT-5382 exhibits meaningful anti-fibrotic activity in a myocardial infarction model

LOXL2 expression is known to be upregulated in cardiac fibrosis models<sup>16,29</sup>. Furthermore, the anti-fibrotic effects of LOXL2 inhibitors have previously been associated with improvements in cardiac function<sup>29</sup>. To evaluate the therapeutic utility of SNT-5382, a myocardial infarction (MI) mouse model was used. This model involves permanent ligation of the left coronary artery, with ischemia confirmed both visually (Supplementary Fig. 3A and B) and by echocardiography (ECHO). After MI, SNT-5382 (14 mg/kg) was given daily by oral gavage for 28 days. Losartan (an angiotensin II receptor antagonist, dosed at 15 mg/kg) was used as a positive pharmacological control<sup>32</sup>. SNT-5382 significantly reduced the collagen volume fraction (reflective of fibrosis) in the region adjacent to the infarct compared to vehicle and losartan treatment groups (Fig. 4A,B). In addition, mature collagen crosslinks (Pyridinoline (PYD)) were reduced by SNT-5382 compared to vehicle, while the collagen content (by hydroxyproline (HYD)) was unaffected (Supplementary Fig. 4A,B) in this acute model. Importantly, SNT-5382 significantly improved cardiac function (measured by ECHO left ventricular ejection fraction (LVEF) and fractional shortening (LVFS)) in the MI model in a paired analysis (Day 1 vs Day 28) and when compared to the vehicle treatment group at 28 days (Fig. 4C,D and Supplementary Fig. 5, respectively). Furthermore, hypertrophy left ventricular end-systolic diameter (LVESD) was also significantly improved by treatment with SNT-5382 (Supplementary Fig. 6). In this experiment, losartan had no significant effect on fibrosis or hypertrophy possibly due to the severity of the insult on cardiac function.

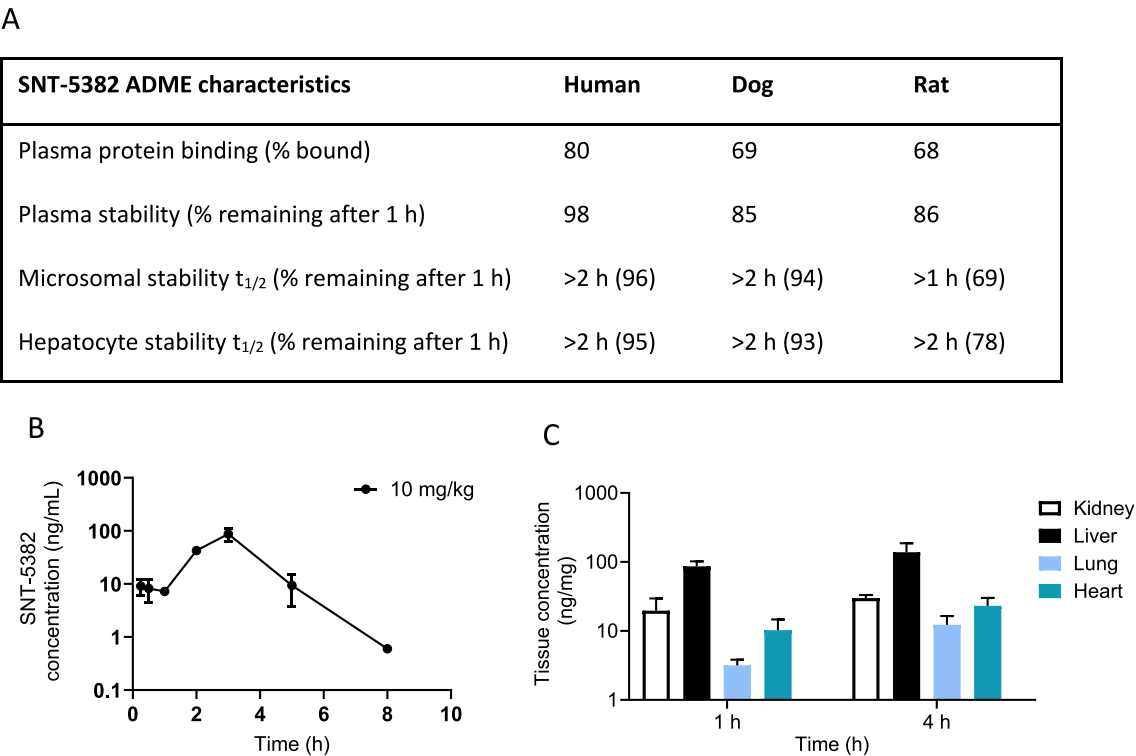


**Fig. 3.** SNT-5382 *in vitro* and *in vivo* ADME characteristics. **(A)** Plasma protein binding, plasma and metabolic (microsomal and hepatocyte) stability across species (human, dog and rat). **(B)** Pharmacokinetic profile of SNT-5382 in male Wistar rats after a single oral dose (10 mg/kg).  $n = 2$  per time-point. **(C)** Tissue distribution at 1 and 4 h post a single oral dose (10 mg/kg) of SNT-5382 in various rat tissues (kidney, liver, lung and heart,  $n = 3$  per time point).



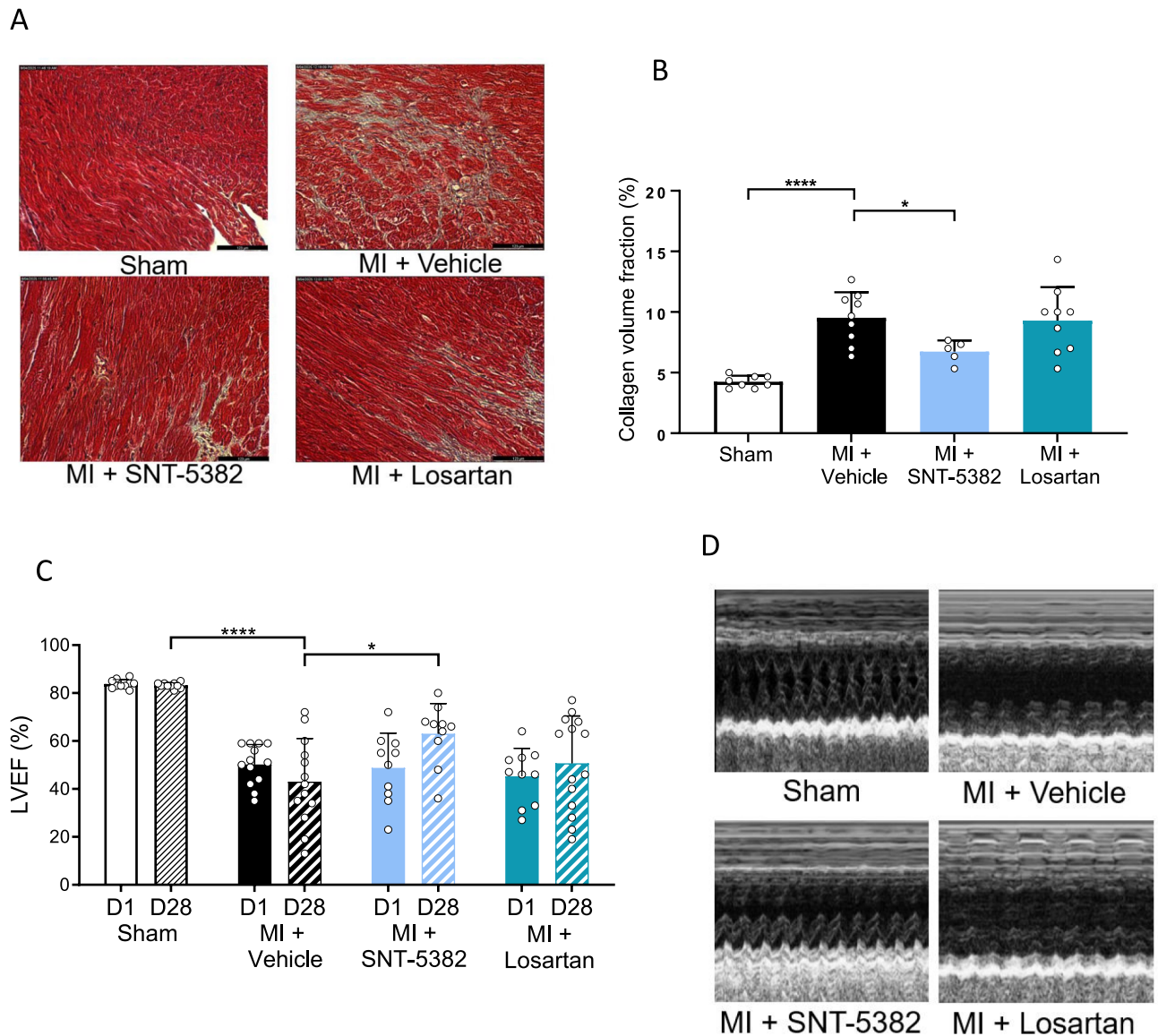


**Fig. 4.** SNT-5382 reduces the area of collagen volume fraction and improves the ejection fraction in a myocardial infarction model. **(A)** Representative histological images of Masson trichrome staining in the region adjacent to the infarct in the myocardial infarction (MI) model at 28 days post-MI. SNT-5382 (14 mg/kg/day as a free base) was dosed orally once daily for 28 consecutive days. Losartan (15 mg/kg) was used as a pharmacological control. The scale bar is equal to 123  $\mu$ m. **(B)** The collagen volume fraction (%) was analysed by the area of Masson trichrome staining in the MI model within the border region of the infarct. Data analysed with one-way analysis of variance (ANOVA) with Dunnett's multiple comparison tests. \* Indicates a significant difference,  $*p < 0.05$ ,  $****p < 0.0001$  vs MI + Vehicle. (n = 5–9 per group). **(C)** The left ventricle ejection fraction (LVEF %) was assessed by echocardiogram taken on Day 1 (D1\_solid bars) and Day 28 (D28\_stripped bars). Data presented as mean  $\pm$  SD (Control) and analysed with one-way analysis of variance (ANOVA) with Brown-Forsythe and Welch ANOVA test comparison tests. \* Indicates a significant difference,  $*p < 0.05$ ,  $****p < 0.0001$  vs Control for same day. (n = 10–14 per group). **(D)** Representative echocardiographic tracings at Day 28 for sham or post-MI mice from either the vehicle, SNT-5382 or losartan treatment groups.

#### SNT-5382 pharmacokinetic and pharmacodynamic profile in healthy subjects

The elevated plasma LOXL2 concentrations in HF patients, together with the promising preclinical anti-fibrotic efficacy and favourable non-clinical PK, pharmacological safety and toxicity studies provided a strong rationale to progress SNT-5382 into a clinical study. A randomized, double-blind, placebo controlled single ascending dose (SAD) and multiple ascending dose (MAD) Phase 1 study was conducted in healthy subjects.

During the SAD study SNT-5382 was very well tolerated, with no serious adverse events reported. Following oral administration of SNT-5382 in a capsule formulation, plasma levels increased in a dose-dependent manner. Peak concentrations occurred 3 h post-dose and were followed by a slow elimination (Fig. 5A). A single dose

of 100 mg achieved an average  $C_{max}$  of 143 ng/mL, equivalent to 0.37  $\mu$ M which is more than 10 $\times$  the human LOXL2  $IC_{50}$ . SNT-5382 exhibits a long terminal half-life of approximately 24 h. Plasma LOXL2 inhibition was examined using an activity-based bioprobe<sup>24</sup>. Peak levels of plasma LOXL2 inhibition (> 85%) were quickly (2 h post dose) reached following a 100 mg oral dose of SNT-5382 (Fig. 5B). Importantly, SNT-5382 sustained high levels of target engagement, with only 26% enzymatic activity recovered after 24 h (Fig. 5C).

SNT-5382 was also well tolerated in the MAD phase when given once a day for 14 days including the following drug-free 7 days until the last visit. Across all three dose cohorts, 31 treatment-emergent adverse events were reported and 29 were mild in severity (2 were moderate). At Day 1, SNT-5382 plasma levels peaked at 3 h after administration, with a terminal half-life ranging from 29.5 to 34.0 h. Accumulation occurred during repeated dosing as expected from the long half-life (Fig. 5D). In line with high plasma concentrations of SNT-5382 high levels of plasma LOXL2 inhibition ( $\geq 85\%$ ) were achieved (Fig. 5E) and sustained. Despite the fast resynthesis rate of LOXL2<sup>24</sup>, recovery of enzymatic activity was negligible (only 6%) when measured 24 h after the last dose (Fig. 5F). Analysis of the PK-PD relationship revealed that desirable high levels of target engagement were reached when SNT-5382 plasma concentrations were approaching or above the *in vitro*  $IC_{50}$  (10 nM) (Fig. 5G). Collectively, these data show that a single daily dose (100 mg) of SNT-5382 meets the requirement of continuous high levels of LOXL2 inhibition and a promising safety profile.

## Discussion

Cardiac fibrosis is a predictor of adverse clinical outcomes for HF patients<sup>4</sup>. The high mortality and morbidity rates associated with HF underscore the clear need for therapies targeting fibrosis, however, few anti-fibrotic approaches have been tested clinically<sup>4,33</sup>. Herein, we link an increase in plasma LOXL2 in HF patients (including patients with AS and HT) with worsening of left ventricular hypertrophy and propose LOXL2 inhibition as a promising therapeutic approach. To this end, we developed and characterized a small molecule, mechanism-based LOXL2 inhibitor, SNT-5382, with excellent drug-like properties. Preclinical studies confirm that SNT-5382 is an anti-fibrotic drug and improves cardiac function. In addition, the Phase 1 study demonstrates a good safety and PK profile, and confirms sustained high levels of target engagement following repeated once-daily oral dosing. All these characteristics establish the therapeutic utility of SNT-5382 in reducing the risk of HF in patients with CVDs.

In this study, patients with HF have elevated plasma LOXL2 concentrations, suggesting circulating LOXL2 may represent a diagnostic and/or prognostic biomarker of myocardial fibrosis. While circulating fibrotic biomarker could improve early detection, monitoring of disease progression, and guide therapeutic interventions<sup>34</sup>, the current gold standard serum biomarker for diagnosis and risk assessment of HF is NT-proBNP, which is a measure of cardiac loading changes rather than fibrosis<sup>17,35</sup>. Therefore, circulating LOXL2 might be an early indicator of ventricular remodeling in the development of CVDs however additional studies in larger cohorts are needed.

Fibrosis progresses when the number of collagen cross-links increases, strengthening collagen fibers. This is associated with increased left ventricular stiffness and, ultimately, a higher risk of hospitalization for HF<sup>36</sup>. SNT-5382 inhibits LOXL2 activity, preventing further cross-link formation. MI model data reveals that LOXL2 inhibition improves cardiac function, likely by reducing ventricular biomechanical stiffness. Moreover, with reduced extracellular matrix accumulation, over time endogenous proteases may resolve existing fibrosis and allow a return to homeostasis. This is consistent with previous clinical studies with the LOXL2 inhibitor GB2064 that demonstrated reduced fibrosis, despite this compound having a more modest LOXL2 target engagement and requiring twice-daily high doses of 1000 mg<sup>22</sup>.

Recent findings explaining the failure of the LOXL2 antibody simtuzumab<sup>23,24</sup> have renewed interest in LOXL2 as an anti-fibrotic target. The association of high levels of LOXL2 in fibrotic tissues and plasma with HF as well as other fibrotic diseases<sup>15</sup>, coupled with the availability of SNT-5382 as a safe and efficacious LOXL2 inhibitor in humans, shall now enables thorough evaluation of its full clinical potential.

## Conclusion

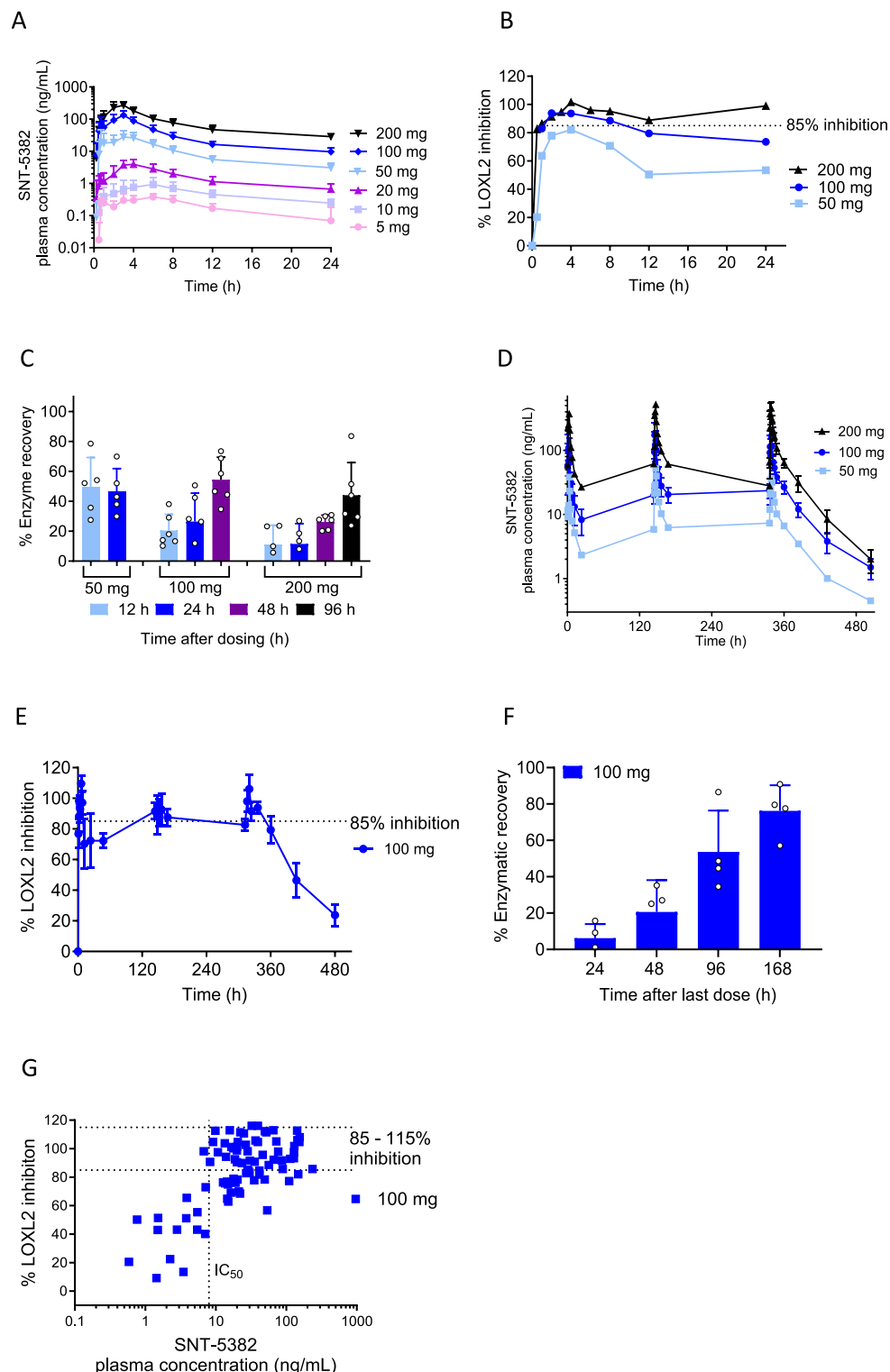
Our study provides strong evidence that LOXL2 inhibition is a promising therapeutic strategy for reducing fibrosis-mediated HF in patients. Elevated circulating LOXL2 levels in HF patients may serve as a potential early indicator of myocardial remodeling. The small molecule LOXL2 inhibitor SNT-5382 reduces fibrosis and improves cardiac function in a preclinical model. In Phase 1 clinical trials SNT-5382 shows a good safety profile with sustained high levels of target engagement. Subsequent studies will be crucial in evaluating the therapeutic efficacy of SNT-5382 in clinical trials for patients with HF.

## Methods

### Subjects

Plasma samples from 36 hypertensive subjects were evaluated. Twenty-three of these patients had been diagnosed with HF. The diagnosis of HF was based on the presence of 1 major and 2 minor Framingham criteria, and was confirmed by echocardiographic alterations in cardiac morphology and function (left ventricular ejection fraction < 50% and/or alterations compatible with diastolic dysfunction) and by the presence of elevated levels of the NT-proBNP (> 125 pg/mL)<sup>37</sup>. Patients were stable and treated when the sample was obtained (Supplementary Table 1). 43.5% of patients were in class II, 52% in class III and 4.5% in class IV. The remaining 13 HT patients without HF were used as control.

Plasma samples were obtained from patients with severe aortic stenosis (AS) and HF (n=12) prior to aortic valve replacement surgery (Supplemental table 1). AS was defined by the presence of an aortic valvular surface < 1 cm<sup>2</sup> and/or medium aortic gradient > 50 mmHg or peak > 60 mmHg and surgical indication of aortic



valve replacement. Plasma samples from 9 control subjects (with no history of cardiovascular disease) were used as controls for this cohort for LOXL2 analyses. Demographic and clinical characteristics of the patients are shown in Supplemental Table 1. The study conformed to the principles of the Helsinki Declaration. All of the subjects provided written consent to participate in the study, and the institutional review committee approved the study protocol.

### LOXL2 plasma concentration and inhibition

The plasma LOXL2 concentration was measured using a LOXL2 sandwich ELISA with Simoa technology (Quanterix) which has a lower limit of detection of 3 pg/mL<sup>24</sup>. The LOXL2 inhibition/ target engagement were measured using an activity based bioprobe<sup>24</sup>.



◀ **Fig. 5.** Pharmacokinetics and pharmacodynamics of SNT-5382 in healthy subjects in clinical studies. (A) SAD study PK profile of SNT-5382 (dose range: 5 mg–200 mg) in healthy male subjects over 24 h.  $n = 6$  per dose. (B) Target engagement in SAD study was measured by an activity-based bioprobe that detects remaining active LOXL2 enzymatic sites available after treatment with SNT-5382 (50, 100 or 200 mg) in the plasma from healthy subjects. The conservative threshold of  $\geq 85\%$  inhibition is based on a 15% assay variation observed at high levels of target engagement ( $n = 5–6$ ). (C) The recovery of LOXL2 enzymatic activity after a single dose (range 50, 100 or 200 mg) of SNT-5382 is shown at 24, 48 and 96 h. (D) Plasma concentrations of SNT-5382 measured in healthy male volunteers ( $n = 6$ ) receiving daily oral doses (range 50, 100 or 200 mg) for 14 consecutive days. (E) Target engagement of SNT-5382 (100 mg) in healthy patients receiving daily dosing for 14 days ( $n = 6$ ). (F) Recovery of LOXL2 enzymatic activity at different times (24, 48, 96 and 168 h) after the last dose of SNT-5382 (100 mg) in the MAD study. (G) Correlation of SNT-5382 plasma concentration with LOXL2 inhibition at dose level of 100 mg in MAD study ( $n = 6$ ).

### Fluorometric enzymatic assays

A standard Amplex red assay was used to determine the level of enzymatic activity for various oxidases. The detailed methodologies for concentration response curves, jump dilution, time-dependency, and the substrate competition assays can be found in previous publication<sup>29</sup>.

Native human LOX was collected from conditioned media of serum starved immortalized human fibroblast cells (IMR90) then fractionated and concentrated in urea for enzymatic assays, as previously described<sup>29</sup>. Human recombinant proteins were purchased [LOXL2 (R&D systems #2639-AO), LOXL3 (R&D systems #6069-AO)] or isolated (LOXL1 and LOXL4r from overexpressing cell lines, kindly supplied by Dr. Fernando Rodríguez Pascual, Spain).

### Off target screen

SNT-5382 was screened at Eurofins Cerep-Panlabs Taiwan, Ltd in the a “SafetyScreen” against 87 macromolecular targets in a standard assay at a test concentration of 10  $\mu$ M.

### In vivo studies

All tprocedures of the study followed ARRIVE guidelines. All animal procedures were approved by the Institutional Animal care and Use committee and conformed to the guide for the care and use of Laboratory Animals published by the U.S. National Institutes of Health (NIH Publication No. 85-23, revised in 1996). Animals were euthanized according to approved IACUC protocols and AVMA guidelines, which involved CO<sub>2</sub> asphyxiation followed by cervical dislocation to confirm death. All the methods were performed in accordance with relevant guidelines and regulations.

### In vivo pharmacokinetics and tissue distribution

Both the PK and tissue distribution studies were performed at Sundia (China). In both studies, male Wistar rats were given a single oral dose of SNT-5382 (10 mg/kg). The concentration of SNT-5382 was measured in the plasma and in the homogenised tissues by high-performance liquid chromatography-mass spectrometry/mass spectrometry LC-MS/MS (API4000 LC-MS/MS) with a lower limit of detection of 1 ng/mL. During the PK studies the plasma was collected at the following times after dosing 0.25, 0.5, 1, 2, 3, 5 and 8 h ( $n = 2$ , per time point). In the tissue distribution study tissues (including: lung, liver, heart and kidney) were harvested at 1 and 4 h and SNT-5382 concentration was determined ( $n = 3$ , per time point).

### In vivo cardiac fibrosis model

Male C57BL/6J wild type mice were from The Jackson Laboratory. They were housed in groups of four to five per cage in a room maintained at  $23 \pm 1$  °C and  $55 \pm 5\%$  humidity with a 12-h light/dark cycle and were given ad libitum access to food and water. At the beginning of experiments, they were 10–11 weeks old.

The myocardial infarction (MI) was performed at CL Laboratory LLC (USA). MI was induced by occluding the left coronary artery, as described previously<sup>38</sup>. Sham mice underwent the same surgery as the MI mice, but were not subjected to coronary artery occlusion. Briefly, mice were anesthetized with ketamine (100 mg/kg) and xylazine (10 mg/kg). Respiration was supported by a small animal ventilator (MiniVent 845, Harvard Apparatus) to standardise electrocardiogram monitoring, which was performed continuously. The left coronary artery was identified visually using a stereo microscope (Stemi 2000C, ZEISS), and a 7–0 suture was placed around the artery approximately 2 mm below the left atrium. Permanent occlusion of the left coronary artery was achieved by ligating it with a suture. The chest was then closed with 6–0 silk suture. Once spontaneous respiration resumed, the endotracheal tube was removed. The animals were monitored until fully conscious. After they were returned to their cages, standard chow and water were provided. At 24 h post-surgery, myocardial ischemia was confirmed by the presence of pallor in the affected region of the heart colour and echocardiography. Mice with fractional shortening between 10 and 40% were included in the study. Total mortality in this study was 28% with more than 65% of these dying in the first 5 days post-surgery. Early and late mortalities occurred in all groups at similar frequency. Mice were treated with daily doses of SNT-5382 (14 mg/kg p.o.), losartan (15 mg/kg) or Vehicle (water) via oral gavage for 4 weeks. All mice were sacrificed 28 days post-surgery. Studies and analysis were performed by investigators blinded to treatments.

## Echocardiography

*In vivo* cardiac function was assessed by transthoracic echocardiography (Acuson P300, 18MHz transducer; Siemens) in conscious mice, as described previously<sup>38</sup>. Using the left ventricular long axis view, M mode ECHO was acquired to determine effects on hypertrophy by measuring the left ventricle end systolic diameter (LVESD). Fractional shortening (FS) was calculated from the end-diastolic diameter (EDD) and end-systolic diameter (ESD) using the following equation:  $FS = [(EDD - ESD)/EDD] \times 100\%$ . Ejection fraction (EF) was calculated from the end-diastolic diameter (EDD) and end-systolic diameter (ESD) using the following equation:  $[(EDD^2 - ESD^2)/EDD^2] \times 100\%$ . Three to five beats were averaged for each mouse. Investigators were blinded to treatments performed in all studies and during analysis. The transthoracic echocardiography was performed at Day 1 and Day 28.

## Measurement of cardiac fibrosis

Adult mouse hearts were fixed with 10% buffered formalin, embedded in paraffin, and cross-sectioned at 6  $\mu$ m, as described previously<sup>38</sup>. One middle longitudinal section per heart was stained with Masson's trichrome to assess fibrosis in the non-infarct area adjacent to the infarct. Fibrotic blue area and whole non-infarct area were measured using computerized planimetry (Image J). The fibrotic area was analysed only on transverse sections and expressed as a percentage of fibrotic area to the whole non-infarct area. Three random fields per heart at  $\times 100$  magnification were evaluated and averaged. A total 24 fields per group were measured in the study. The observer was blinded to the treatment group during the analysis of the cardiac sections. Representative images were taken of the non-infarct area taken adjacent to the boarder of the infarct area.

## Measurement of collagen content (hydroxyproline) and crosslinking (Pyridinoline)

The MI model heart tissue was flash frozen in liquid nitrogen. The MI + Vehicle and MI + SNT-5382 samples were homogenised and approximately 15mg was freeze-dried and then reduced with NABH<sub>4</sub>. The pellet was hydrolysed in 6 mol/L HCl at 100 °C for 24h. Hydroxyproline and Pyridinoline were extracted from the hydrolysate using a solid phase extraction system (Gilson GX-271 ASPECA system). After extraction and drying, the samples were analysed by UHPLC-ESI-MS/MS on a Thermo Dionex UHPLC and TSQ Endura triple quad mass spectrometer. Total protein was quantified in the samples using a commercially available kit (Quick Zyme Biosciences, Leiden, The Netherlands). For further details on extraction and detection please see reference<sup>29</sup>. Data presented as mean  $\pm$  SD and analysed with Unpaired t test with Welch's correction. (n = 10–12 per group).

## Statistical analysis

Differences between patient groups or between different condition in *in vitro* studies, were analysed by a Student's t-test for unpaired normally distributed data. If a F-test was significant, then an unpaired t-test with Welch's correction was used. For all other data Mann-Whitney U test was used. The correlation between continuously distributed variables was tested by correlation coefficients and univariate regression analysis. A value of  $p < 0.05$  was considered statistically significant. The differences across groups in *in vivo* studies were analysed using a one-way ANOVA if normality was established, otherwise a Brown-Forsythe and Welch ANOVA was completed with a Dunnett's T3 multiple comparison test. To compare the Day 1 and Day 28 data for the *in vivo* studies a paired two tailed T-test was used, if normality was not demonstrated a non-parametric Wilcoxon test was used. Values are expressed as mean  $\pm$  SD. The analysis of the patient plasma samples an analysis of Covariance (ANCOVA) was performed to evaluate the differences across groups while statistically controlling for the influence of relevant covariables. The assumptions of homogeneity of regression of slopes, normality, homoscedasticity and independence of residuals were verified.

## Clinical studies

A randomized, double blind, placebo-controlled SAD and MAD study was completed in healthy male subjects to evaluate SNT-5382. In the SAD study, cohorts of 6 healthy male subjects received a single dose of SNT-5382 at one of the following doses: 5, 10, 20, 50, 100 or 200 mg. Another two subjects received placebo in each cohort. In the MAD study, three cohorts with 6 healthy subjects received daily doses 50 mg or 100 mg or 200 mg of SNT-5382 for consecutive 14 days. Another two subjects received placebo in each cohort. The plasma samples, for the SAD and MAD studies were taken at pre-dose and 0.25, 0.5, 0.75, 1, 2, 3, 4, 6, 8, 12, 24, 48, 72, 96 h. For the MAD trial additional plasma samples were collected on days 7 and 14 at the time intervals previously mentioned. For high levels of target engagement, a conservative estimate of intrinsic variation was set at 15%.

All subjects completed the study in accordance with the protocol.

## Data availability

All data generated or analysed during this study are included in this published article.

Received: 16 January 2025; Accepted: 9 June 2025

Published online: 02 July 2025

## References

1. Hinderer, S. & Schenke-Layland, K. Cardiac fibrosis—A short review of causes and therapeutic strategies. *Adv. Drug Deliv. Rev.* **146**, 77–82. <https://doi.org/10.1016/j.addr.2019.05.011> (2019).
2. Castrichini, M. et al. Clinical impact of myocardial fibrosis in severe aortic stenosis. *Eur. Heart J. Suppl.* **23**, E147–E150. <https://doi.org/10.1093/eurheartj/suab120> (2021).
3. Gerds, E. Left ventricular structure in different types of chronic pressure overload. *Eur. Heart J. Suppl.* **10**, E23–E30. <https://doi.org/10.1093/eurheartj/sun015> (2008).

4. Ravassa, S. et al. Cardiac Fibrosis in heart failure: Focus on non-invasive diagnosis and emerging therapeutic strategies. *Mol. Asp. Med.* **93**, 101194. <https://doi.org/10.1016/j.mam.2023.101194> (2023).
5. Wells, R. G. Tissue mechanics and fibrosis. *Biochim. Biophys. Acta* **1832**, 884–890. <https://doi.org/10.1016/j.bbadis.2013.02.007> (2013).
6. Brower, G. L. et al. The relationship between myocardial extracellular matrix remodeling and ventricular function. *Eur. J. Cardiothorac. Surg.* **30**, 604–610. <https://doi.org/10.1016/j.ejcts.2006.07.006> (2006).
7. Lopez, B. et al. Impact of treatment on myocardial lysyl oxidase expression and collagen cross-linking in patients with heart failure. *Hypertension* **53**, 236–242. <https://doi.org/10.1161/HYPERTENSIONAHA.108.125278> (2009).
8. Kasner, M. et al. Diastolic tissue Doppler indexes correlate with the degree of collagen expression and cross-linking in heart failure and normal ejection fraction. *J. Am. Coll. Cardiol.* **57**, 977–985. <https://doi.org/10.1016/j.jacc.2010.10.024> (2011).
9. Perez Del Villar, C. et al. Impact of acute hypertension transients on diastolic function in patients with heart failure with preserved ejection fraction. *Cardiovasc. Res.* **113**, 906–914. <https://doi.org/10.1093/cvr/cvx047> (2017).
10. Lopez, B., Querejeta, R., Gonzalez, A., Larman, M. & Diez, J. Collagen cross-linking but not collagen amount associates with elevated filling pressures in hypertensive patients with stage C heart failure: potential role of lysyl oxidase. *Hypertension* **60**, 677–683. <https://doi.org/10.1161/HYPERTENSIONAHA.112.196113> (2012).
11. Zile, M. R. et al. Myocardial stiffness in patients with heart failure and a preserved ejection fraction: Contributions of collagen and titin. *Circulation* **131**, 1247–1259. <https://doi.org/10.1161/CIRCULATIONAHA.114.013215> (2015).
12. Lopez, B. et al. Myocardial collagen cross-linking is associated with heart failure hospitalization in patients with hypertensive heart failure. *J. Am. Coll. Cardiol.* **67**, 251–260. <https://doi.org/10.1016/j.jacc.2015.10.063> (2016).
13. Bornstein, A. B., Rao, S. S. & Marwaha, K. *Left Ventricular Hypertrophy*. (2024).
14. Yancy, C. W. et al. 2017 ACC/AHA/HFSA focused update of the 2013 ACCF/AHA guideline for the management of heart failure: A report of the American college of cardiology/American heart association task force on clinical practice guidelines and the heart failure society of America. *J. Am. Coll. Cardiol.* **70**, 776–803. <https://doi.org/10.1016/j.jacc.2017.04.025> (2017).
15. Yang, N., Cao, D. F., Yin, X. X., Zhou, H. H. & Mao, X. Y. Lysyl oxidases: Emerging biomarkers and therapeutic targets for various diseases. *Biomed. Pharmacother.* **131**, 110791. <https://doi.org/10.1016/j.biopha.2020.110791> (2020).
16. Yang, J. et al. Targeting LOXL2 for cardiac interstitial fibrosis and heart failure treatment. *Nat. Commun.* **7**, 13710. <https://doi.org/10.1038/ncomms13710> (2016).
17. Zhao, Y. et al. Increased serum lysyl oxidase-like 2 levels correlate with the degree of left atrial fibrosis in patients with atrial fibrillation. *Biosci. Rep.* **37**, BSR20171332. <https://doi.org/10.1042/BSR20171332> (2017).
18. Johnson, R. et al. Identification of potential biomarkers for predicting the early onset of diabetic cardiomyopathy in a mouse model. *Sci. Rep.* **10**, 12352. <https://doi.org/10.1038/s41598-020-69254-x> (2020).
19. Stepan, J. et al. Lysyl oxidase-like 2 depletion is protective in age-associated vascular stiffening. *Am. J. Physiol. Heart Circ. Physiol.* **317**, H49–H59. <https://doi.org/10.1152/ajpheart.00670.2018> (2019).
20. Wang, H. et al. Sex differences and role of lysyl oxidase-like 2 in angiotensin II-induced hypertension in mice. *Am. J. Physiol. Heart Circ. Physiol.* **327**, H642–H659. <https://doi.org/10.1152/ajpheart.00110.2024> (2024).
21. Stepan, J. et al. LOXL2 inhibition ameliorates pulmonary artery remodeling in the pulmonary hypertension. (2023). <https://doi.org/10.1101/2023.10.24.563874>
22. Verstovsek, S. M. J., Rampal R., Cilloni D., Harrison C.N., Jacoby B., Slack R.J., Aslanis V., Singh B. & Lindmark B. *MYLOX-1: An Open-Label, Phase IIa Study of the Safety, Tolerability, Pharmacokinetics, and Pharmacodynamics of Oral LOXL2 Inhibitor, GB2064, in Myelofibrosis: Intermediate Assessment*, <https://ir.galecto.com/static-files/881fe7e2-b15e-42bf-81e5-1bda02edd13b> (2022).
23. Bell, J. A. et al. Spatial transcriptomic validation of a biomimetic model of fibrosis enables re-evaluation of a therapeutic antibody targeting LOXL2. *Cell Rep. Med.* <https://doi.org/10.1016/j.xcrmm.2024.101695> (2024).
24. Findlay, A. et al. An activity-based bioprobe differentiates a novel small molecule inhibitor from a LOXL2 antibody and provides renewed promise for anti-fibrotic therapeutic strategies. *Clin. Transl. Med.* **11**, 10. <https://doi.org/10.1002/ctm2.572> (2021).
25. Chien, J. W. et al. Serum lysyl oxidase-like 2 levels and idiopathic pulmonary fibrosis disease progression. *Eur. Respir. J.* **43**, 1430–1438. <https://doi.org/10.1183/09031936.00141013> (2014).
26. Muir, A. J. et al. Serum LYSYL oxidase-like-2 (SLOXL2) levels correlate with disease severity in patients with primary sclerosing cholangitis. *J. Hepatol.* [https://doi.org/10.1016/s0168-8278\(16\)00694-2](https://doi.org/10.1016/s0168-8278(16)00694-2) (2016).
27. Zhu, Z. Serum LOXL2 is elevated and an independent biomarker in patients with coronary artery disease. *Int. J. Gener. Med.* **17**, 4071–4080. <https://doi.org/10.2147/ijgm.S478044> (2024).
28. Findlay, A. D. et al. Identification and optimization of mechanism-based fluoroalkylamine inhibitors of LYSYL oxidase-like 2/3. *J. Med. Chem.* **62**, 9874–9889. <https://doi.org/10.1021/acs.jmedchem.9b01283> (2019).
29. Schilter, H. et al. The lysyl oxidase like 2/3 enzymatic inhibitor, PXS-5153A, reduces crosslinks and ameliorates fibrosis. *J. Cell Mol. Med.* **23**, 1759–1770. <https://doi.org/10.1111/jcmm.14074> (2019).
30. Foot, J. S. et al. PXS-4681A, a potent and selective mechanism-based inhibitor of SSAO/VAP-1 with anti-inflammatory effects in vivo. *J. Pharmacol. Exp. Ther.* **347**, 365–374. <https://doi.org/10.1124/jpet.113.207613> (2013).
31. Ma, H. Y. et al. LOXL4, but not LOXL2, is the critical determinant of pathological collagen cross-linking and fibrosis in the lung. *Sci. Adv.* **9**, eadf0133. <https://doi.org/10.1126/sciadv.adf0133> (2023).
32. Diez, J. et al. Losartan-dependent regression of myocardial fibrosis is associated with reduction of left ventricular chamber stiffness in hypertensive patients. *Circulation* **105**, 2512–2517. <https://doi.org/10.1161/01.cir.0000017264.66561.3d> (2002).
33. Black, N. et al. Remote myocardial fibrosis predicts adverse outcome in patients with myocardial infarction on clinical cardiovascular magnetic resonance imaging. *J. Cardiovasc. Magn. Reson.* <https://doi.org/10.1016/j.jocmr.2024.101064> (2024).
34. Zhu, L., Wang, Y., Zhao, S. & Lu, M. Detection of myocardial fibrosis: Where we stand. *Front. Cardiovasc. Med.* <https://doi.org/10.3389/fcvm.2022.926378> (2022).
35. Liu, C. Y. et al. Association of elevated NT-proBNP with myocardial fibrosis in the multi-ethnic study of atherosclerosis (MESA). *J. Am. Coll. Cardiol.* **70**, 3102–3109. <https://doi.org/10.1016/j.jacc.2017.10.044> (2017).
36. Gonzalez, A., Lopez, B., Ravassa, S., San Jose, G. & Diez, J. The complex dynamics of myocardial interstitial fibrosis in heart failure Focus on collagen cross-linking. *Biochim. Biophys. Acta Mol. Cell Res.* **1866**, 1421–1432. <https://doi.org/10.1016/j.bbamcr.2019.06.001> (2019).
37. Ponikowski, P. et al. 2016 ESC Guidelines for the diagnosis and treatment of acute and chronic heart failure: The task force for the diagnosis and treatment of acute and chronic heart failure of the European Society of Cardiology (ESC) Developed with the special contribution of the Heart Failure Association (HFA) of the ESC. *Eur. Heart J.* **37**, 2129–2200. <https://doi.org/10.1093/eurheartj/ehw128> (2016).
38. Parajuli, N., Yuan, Y., Zheng, X., Bedja, D. & Cai, Z. P. Phosphatase PTEN is critically involved in post-myocardial infarction remodeling through the Akt/interleukin-10 signaling pathway. *Basic Res. Cardiol.* **107**, 248. <https://doi.org/10.1007/s00395-012-0248-6> (2012).

## Acknowledgements

The authors would like to thank Synairgen for collaborating on the Phase 1 studies. We would also like to acknowledge the following previous employees for their contribution to the development of SNT-5382: Yimin Yao, Alberto Buson, Heidi Schilter, Angelique Greco, Joshua Moses, Tin Yow, Mandar Deodhar. We are grateful

to Dr. Fernando Rodríguez Pascual, Universidad Autónoma de Madrid, Spain, for the provision of LOXL1 and LOXL4 reagents.

### Author contributions

The following authors made a substantial contribution to the conception WJ, AF, JF, CT, BC, AG; the acquisition and analysis and interpretation of data LP, AF, JB, BC, JF, RH, DH, AJ, JS, CT, AZ, WZ, BL, SR, AG, WJ; have drafted the work or substantively revised it LP, BC, AF, JF, DH, AG, WJ.

### Funding

This study was supported by Syntara.

### Declarations

### Competing interests

The following authors Lara Perryman, Alison Findlay, Jonathan Foot, Amar Joshi, Amna Zahoor, Craig Turner, Dieter Hamprecht, Jana Baskar, Jessica Stolp, Ross Hamilton, Wenbin Zhou, Brett Carlton and Wolfgang Jarolimek have been employees of Syntara (the company that owns SNT-5382) or its predecessor, Pharmaxis, and the staff have stocks in the company. The remaining authors have no competing interests to declare. All authors have read and approved the manuscript.

### Ethics approval and consent to participate

The study conformed to the principles of the Helsinki Declaration. All of the subjects provided written consent to participate in the study, and the Universidad the Navarra committee approved the study protocol.

### Consent for publication

We confirm that all authors have read and approved this manuscript for submission. Furthermore, we affirm that the content of this manuscript has not been published or submitted for publication elsewhere.

### Human and animal participants

All animal procedures were approved by the Institutional Animal care and Use committee and conformed to the guide for the care and use of Laboratory Animals published by the U.S. National Institutes of Health (NIH Publication No. 85–23, revised in 1996).

### Additional information

**Supplementary Information** The online version contains supplementary material available at <https://doi.org/10.1038/s41598-025-06312-2>.

**Correspondence** and requests for materials should be addressed to W.J.

**Reprints and permissions information** is available at [www.nature.com/reprints](http://www.nature.com/reprints).

**Publisher's note** Springer Nature remains neutral with regard to jurisdictional claims in published maps and institutional affiliations.

**Open Access** This article is licensed under a Creative Commons Attribution-NonCommercial-NoDerivatives 4.0 International License, which permits any non-commercial use, sharing, distribution and reproduction in any medium or format, as long as you give appropriate credit to the original author(s) and the source, provide a link to the Creative Commons licence, and indicate if you modified the licensed material. You do not have permission under this licence to share adapted material derived from this article or parts of it. The images or other third party material in this article are included in the article's Creative Commons licence, unless indicated otherwise in a credit line to the material. If material is not included in the article's Creative Commons licence and your intended use is not permitted by statutory regulation or exceeds the permitted use, you will need to obtain permission directly from the copyright holder. To view a copy of this licence, visit <http://creativecommons.org/licenses/by-nc-nd/4.0/>.

© The Author(s) 2025